Journal of Materials Chemistry C

Accepted Manuscript

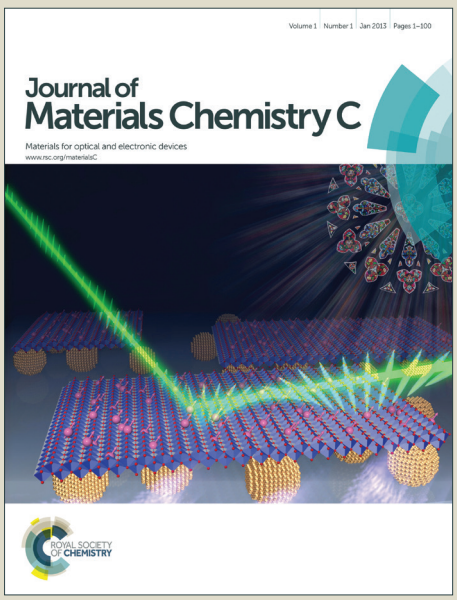

ROYAL SOCIETY OF CHEMISTRY

www.rsc.org/materialsC

The role of phase morphology on the nature of long-lived charges in semiconductor polymer:fullerene systems

Fei Dou,[a,b,c] Ester Buchaca-Domingo,[b,e] Maciej Sakowicz,[a] Elham Rezasoltani,[a] Thomas McCarthy-Ward,[d] Martin Heeney,[d] Xinping Zhang,[c] Natalie Stingelin,[b] Carlos Silva[a,f]

[a] Département de physique & Regroupement québécois sur les matériaux de pointe, Université de Montréal, Caisse postale 6128, Succursale centre-ville, Montréal (Québec) H3C 3J7, Canada. Tel: (514) 343-2364; E-mail: carlos.silva@umontreal.ca

[b] Department of Materials and Centre for Plastic Electronics, Imperial College London, South Kensington Campus, London, SW7 2AZ, United Kingdom.

[c] Institute of Information Photonics Technology and College of Applied Sciences, Beijing University of Technology, Beijing 100124, P. R. China.

[d] Department of Chemistry and Centre for Plastic Electronics, Imperial College London, South Kensington Campus, London, SW7 2AZ, United Kingdom.

[e] Division of Physical Sciences and Engineering, Solar and Photovoltaic Engineering Research Center, King Abdullah University of Science and Technology (KAUST), Thuwal, Saudi Arabia.

[f] Visiting Professor, Department of Physics, Imperial College London, South Kensington Campus, London, SW7 2AZ, United Kingdom.

In this work, we investigate the role of phase morphology on the nature of charges in poly(2,5-bis(3-tetradecyl-thiophen-2-yl)thieno[3,2,-b]thiophene) (pBTTT-C_{16}) and phenyl-C_{61}-butyric acid methyl ester ($PC_{61}BM$) blends over timescales greater than hundreds of microseconds by quasi-steady-state photoinduced absorption spectroscopy. Specifically, we compare an essentially fully intermixed, one-phase system based on a 1:1 (by weight) pBTTT-C_{16}:$PC_{61}BM$ blend, known to form a co-crystal structure, with a two-phase morpholgy composed of relatively material-pure domains of the neat polymer and neat fullerene. The co-crystal occurs at a composition of up to 50 wt% $PC_{61}BM$, because pBTTT-C_{16} is capable of hosting fullerene derivatives such as $PC_{61}BM$ in cavities between its side chains. In contrast, the predominantly two-phase system can be obtained by manipulating a 1:1 polymer:fullerene blend with the assistance of a fatty acid methyl ester (dodecanoic acid methyl ester, Me12) as additive, which hinders co-crystal formation. We find that triplet excitons and polarons are generated in both phase morphologies. However, polarons are generated in the predominantly two-phase system at higher photon energy than for the structure based on the co-crystal phase. By means of a quasi-steady-state solution of a mesoscopic rate model, we demonstrate that the steady-state polaron generation efficiency and recombination rates are higher in the finely intermixed, one-phase system compared to the predominantly phase-pure, two-phase morphology. We suggest that the polarons generated in highly intermixed structures, such as the co-crystal investigated here, are localised polarons while those generated in the phase-separated polymer and fullerene systems are delocalised polarons. We expect this picture to apply generally to other organic-based heterjunctions of complex phase morphologies including donor:acceptor systems that form, for instance, molecularly mixed amorphous solid solutions, underlining the generality of the understanding gained here.

1. Introduction

The optical and electronic properties of polymer:fullerene blends for use as light-harvesting layer in organic photovoltaic (OPV) cells are strongly dictated by various structural features of the active layer, including the extend of intermixing, vertical phase segregation, domain size and, generally, its phase morphology. The number of phases present, the nature of phases, and the phase distribution are important characteristics of the phase morphology. [1, 2] Therefore, detailed knowledge of how these structural attributes define charge generation and recombination environments is fundamental to gain a detailed picture of the optoelectronic landscape of such architectures and to further enhance the performance of polymer:fullerene solar cells. [3, 4] Here, we will focus on the nature of long-lived photoexcitations generated in pBTTT-C_{16}:$PC_{61}BM$ blends. The polymer pBTTT-C_{16} is an electron-donor material with respect to fullerene derivatives, which in the solid state is semicrystalline and also displays relatively high hole mobilities when measured in field-effect transistors. [5-7] Moreover, it has been demonstrated that pBTTT-C_{16} shows a high PL quenching efficiency (>90%) when blended with $PC_{61}BM$ resulting from co-crystallisation of the two components. [8] This co-crystal formation makes pBTTT-C_{16}:$PC_{61}BM$ an ideal model system to control the type and amount of phases, e.g. by changing the type of fullerene, by tuning the composition ratios between two components, [9-15] or use of additives such as fatty acid methyl ester [16] — a strategy exploited here. Phase morphology control is important as it permits to establish certain structure/property interrelationships. Jamieson *et al.* correlated, for instance, the resulting device performance with the formation of relatively phase-pure PCBM domains. [15] Buchaca-Domingo *et al*. demonstrated moreover a dependency of exciton decay dynamics and charge generation, as measured in transient-absorption spectroscopy and microwave photoconductivity measurements, with the extent of intermixing/phase separation. [16] In

agreement with this picture, Scarongella *et al*. found higher electron and hole transfer rates, and as a consequence a higher generation of free charges, in structures where highly intermixed phases co-existed with relatively material-pure domains of PCBM. [17]

We exploit here pBTTT-C_{16}:$PC_{61}BM$ blends to gain further insight in this dependence of photoinduced charge generation and recombination on phase morphology. We focus on two specific structures: *i*) 1:1 pBTTT-C_{16}:$PC_{61}BM$ binaries, which lead to an ordered intermixed phase (the co-crystal phase) with minimal phase-pure domains forming; and *ii*) a predominantly two-phase system, realised using a ternary blend comprising pBTTT-C_{16}, $PC_{61}BM$ and dodecanoic acid methyl ester, Me12, where more than 80% of $PC_{61}BM$ is expelled from the matrix of the polymer because of the presence of this additive, leading to an increased amount of phase-pure pBTTT-C_{16} and fullerene regions. [16-18] By means of quasi-steady-state photoinduced absorption (PIA) spectroscopy, we probe polaron and triplet-exciton generation and recombination kinetics in these different phase morphologies. We carry out most of this work at 10 K, which is a temperature at which we do not expect to generate mobile carriers as suggested in some transient absorption studies carried out at room temperature, [14,19] but rather polarons that are largely localised close to where they were generated. We model the quasi-steady-state population as a function of excitation-laser intensity and modulation frequency to extract kinetic information in the two morphologies, and we consider the photoinduced absorption lineshape in order to compare the nature of photoexcitations in these.

2. Experimental details

One-phase systems were produced from 1:1 (by weight) pBTTT-C_{16}:$PC_{61}BM$ binaries, deposited from 1,2-ortho-dichlorobenzene (1,2-*o*DCB, Aldrich; 20 mg/mL total solute

content). Two-phase structures were induced by adding dodecanoic acid methyl ester (Me12) (10 molar equivalents per monomer unit of the polymer) into such 1:1 (by weight) pBTTT:$PC_{61}BM$/1,2-*o*DCB base-solutions before casting, as described in detail in Ref. 16. Thereby, a pBTTT-C_{16} was employed of a weight-average molecular weight (M_w) of 66 kg/mol and number average molecular weight (M_n) of 34 kg/mol, as measured by gel permeation chromatography (chlorobenzene at 80°C) against polystyrene standards. $PC_{61}BM$ was purchased from Solenne and used as received, and the dodecanoic acid methyl ester (Me12) additives were purchased from Aldrich.

Quasi-steady-state photoinduced absorption (PIA) spectroscopy setup was performed as described elsewhere. [20] In brief, the sample was mounted in a closed-cycle cryostat with the exchange gas at 10 K, and pumped with a 532-nm continuous-wave laser modulated at a frequency f_{pump}=170 Hz. The probe beam consisted of a monochromated 150-W halogen-tungsten lamp, which was modulated at frequency f_{probe}=139 Hz. A Si/PbS dual photoreceiver or a Si avalanche photodiode was used as the detector. The fractional change in transmission of the probe, ΔT, was measured as a function of probe photon energy using a lock-in amplifier (SRS SR830) referenced to the sum frequency ($f_{pump}+f_{probe}$), with the phase set to maximise the PIA signal in the X-channel (in-phase channel). The transmission of the probe through the sample, T, was measured with a second lock-in amplifier (SRS SR810) referenced to f_{probe}. The ratio of these two is the PIA signal, $\Delta T/T$. For frequency dependent PIA measurements, the ΔT was carried out in a single modulation mode (f_{pump}), in which f_{pump} was varied between 1 Hz and 3 kHz without modulation of the probe beam, and T was measured separately by modulating the probe beam with the pump laser blocked. The photoluminescence background was subtracted from the measured ΔT, which was measured by blocking the probe beam.

3. Results and analysis

We applied quasi-steady-state PIA spectroscopy to explore directly the generation of long-lived photoexcitations in the finely intermixed, one-phase pBTTT-C_{16}:$PC_{61}BM$ binaries, as well as the predominantly two-phase systems formed by pBTTT-C_{16}:Me12:$PC_{61}BM$, where the polymer and fullerene are phase separated. The PIA spectra for the one-phase system at 10 K (a) and at room temperature (b) are displayed in Fig. 1. At 10 K (Fig. 1(a)), there are two obvious features: a narrow feature centred at 1.2 eV and a broad feature peaked at 1.4 eV. Furthermore, there is a weak peak in the infrared (IR) region at about 0.6 eV. We attribute the higher energy (1.4 eV) and IR (~0.6 eV) signatures to polaron absorption based on assignments derived from early PIA measurements on regioregular poly(3-hexylthiophene) (P3HT). [21, 22] This assignment is supported by comparing our data with data reported on other conjugated polymers, including ladder-type poly-*para*-phenylene (mLPPP) [23], oligothiophenes [24], and polyfluorene derivatives (PFO) [26], which all display broad polaron absorption features in the visible range. Such an assignment is also in good agreement with reported transient absorption data (TA; 625nm~1000nm) [17] and charge modulation spectroscopy (CMS) data [25] for pBTTT:$PC_{61}BM$ systems. Furthermore, implementing photoinduced-absorption-detected magnetic resonance (DMR) techniques [23-25], previous reports distinguish between the triplet exciton absorption from the polaron absorption in this range of polymers. This earlier body of work allows us to assign the 1.2-eV photoinduced absorption to that of triplet excitons. Similar signatures were also found for regiorandom polythiophene (RRa-P3HT), where the dominant long-lived photoexcitations were attributed to triplets (PIA band at 1.5 eV), while additional PIA bands (0.5 eV and 1.7 eV) were assigned to polarons. [21] Pochas and Spano have studies the nature of these

transitions theoretically using a disordered Holstein Hamiltonian and assign the intra- and intermolecular contribution to the spectral signatures. [27] At room temperature (Fig. 1(b)), we can also observe these three features, but the overall intensity decreases by roughly one order of magnitude compared to that at 10 K with respect to room temperature, while the spectral lineshape is similar at both temperatures. The spectral similarities at low and room temperature suggests that the generation efficiencies of both species are not highly temperature dependent, which can be rationalised by the fact that charge generation occurs with high driving force in these systems, and that intersystem crossing, arising from spin-orbit coupling, does not depend strongly on temperature. Similarly, the lifetime of the relevant species should not display strong temperature dependence for the spectral lineshape to change weakly with temperature. Triplet recombination is governed by Dexter-type transport, which shows weak temperature dependence. [28] Finally, of crucial significance for the rest of this paper, the charges that are probed at quasi-steady state in our experiments are those that are highly localised such that they are most likely to recombine by tunnelling to nearby acceptor sites. [29] These dynamics are also weakly temperature dependent if they do not require activated transport but only tunnelling.

Fig. 1(c) shows the PIA spectrum of the two-phase pBTTT-C_{16}:Me12:$PC_{61}BM$ systems measured at 10 K. In contrast to the spectrum of the finely intermixed pBTTT-C_{16}:$PC_{61}BM$ blend structure (shown in Fig. 1(a)), the high-energy polaron absorption peaked at 1.7 eV is blue-shifted by ~300 meV. We observe a similar phenomenon for the IR peak, which is slightly blue-shifted from 0.60 eV to 0.65 eV. The spectral line shape at room temperature (shown in Fig. 1(d)) is qualitatively similar to that at 10 K but the intensity of all features decreases compared to that at 10 K. However, this decrease is less than that in the finely intermixed systems, indicating different recombination and/or generation processes in these

two different phase morphologies. Furthermore, the peak signal ratio of high-energy polarons to triplet excitons is higher in the two-phase systems. We also find that the shape of the polaron band for the two morphologies is also different in different morphologies. For the one-phase system, a broader tail appears at high energy. We speculate that inhomogeneous broadening effects are more significant in the two-phase system, and we ascribe differences to the spectral lineshape to this.

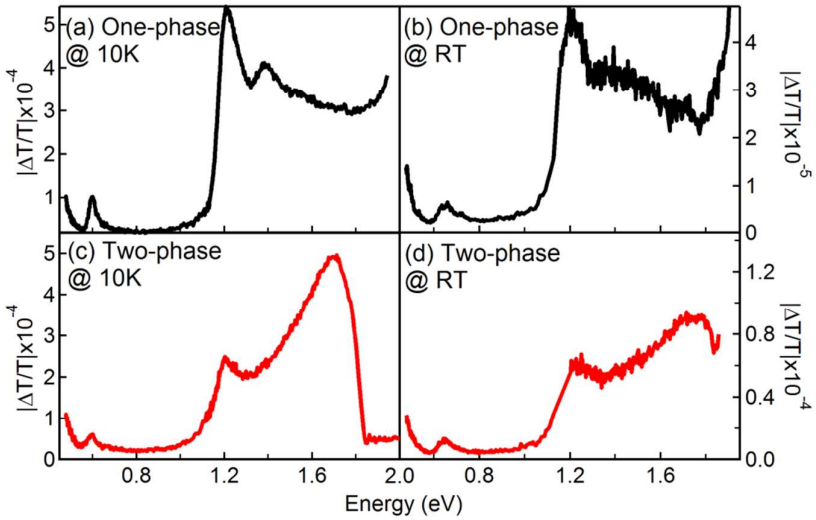

Fig. 1 PIA spectra (X-channel) of a finely mixed, one-phase system formed by pBTTT-C_{16}:$PC_{61}BM$ and a morphology composed of pBTTT-C_{16}:Me12:$PC_{61}BM$ featuring predominantly phase-pure domains of the two components, measured at 10 K (a) and (c), and at room temperature (RT) (b) and (d), respectively.

To explore the generation and recombination kinetics of triplet excitons and polarons in these two different phase morphologies, we performed frequency dependent PIA measurements, which are shown in Fig. 2. We plot the amplitude of the PIA signal as a function of pump modulation frequency for both the high-energy polaron and triplet signatures. The data were measured at the peak of triplet excitons and polarons features at 10 K and normalised to the corresponding values measured from double modulation PIA measurement with the pump modulated at a frequency of 170 Hz and the probe at a frequency of 139 Hz.

For both triplet excitons (Fig.2 (a)) and polarons (Fig.2 (b)), the PIA signal depends weakly on pump modulation frequency at low frequencies, but decreases sharply at higher frequencies. Conceptually, given an effective photoexcitation lifetime τ, if $\omega\tau<1$, ω is the modulation angular frequency, the photoexcitation density varies weakly with ω since τ is shorter compared to the modulation period and the population is close to a steady state. On the other hand when $\omega\tau\approx1$, the signal decreases more prominently with increasing ω, as the effective lifetime is now longer compared to the modulation period, and a true steady state is not achieved [30-33].

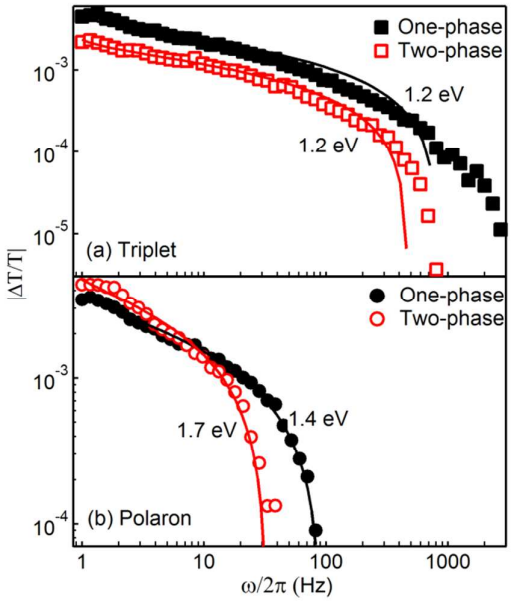

Fig. 2 Frequency dependence of the magnitude of the PIA signal for triplet excitons (a) and polarons (b) in, respectively, finely intermixed pBTTT-C_{16}:$PC_{61}BM$ binaries and phase-separate pBTTT-C_{16}:Me12:$PC_{61}BM$ systems, measured at 10 K. The data was collected at probe photon energies indicated adjacent to the data. The continuous lines through the data are fits using equation (3) and the parameters extracted from the analysis are displayed in Table 1 (see text for details).

We can also observe that triplet excitons in the two systems follow the same trend as polarons and with a transition away from steady state occurring at higher pump modulation frequency. This means that the triplet excitons have a shorter lifetime than the polarons in both systems. Furthermore, the polaron signal (1.7-eV feature) found in the systems dominated by relatively phase-pure domains decays at lower frequency than that (1.4-eV feature) in finely intermixed one-phase structures, which implies that the polarons in the two-phase systems have longer lifetime than the polarons in the finely intermixed one-phase morphologies.

In order to explore the recombination dynamics of polarons and triplets, we undertook pump-intensity dependent PIA measurements. The data in Fig. 3 were measured with a pump modulation frequency of 170 Hz at 10 K, and were normalized to the corresponding values obtained in double modulation PIA measurements using a pump modulation of 170 Hz, a probe modulation of 139 Hz and a pump intensity of 128 mW/cm^2. The PIA signal shows linear dependence at low pump intensity, which evolves to a sub-linear dependence at high intensity for all the species. This implies that unimolecular and bimolecular recombination processes are active in both phase morphologies. [34]

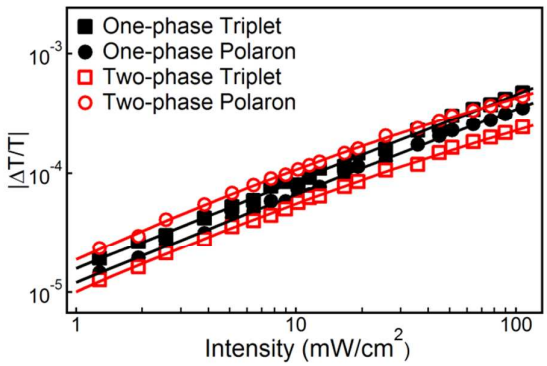

Fig. 3 Pump intensity dependence of the magnitude of the PIA signal. The data was collected at probe photon energies of 1.2 eV, 1.4 eV and 1.7 eV at 10K. The continuous lines are fits to the polynomial function $y=a+bx+cx^2$, where the quadratic term is not equal to zero for both phase morphologies.

The long-lived photoexcitations dynamics in PIA experiment can be described by [32, 33]

$$\frac{dn}{dt} = \kappa\rho G(\omega, t) - \gamma n - \beta n^2, \quad (1)$$

where n is the population density of photogenerated species (triplets or polarons), κ is the quasi-steady-state photogeneration efficiency with respect to the absorbed photons, ρ is the density of pump photons per unit volume and per unit time, G is a periodic function describing the pump-laser modulation, and γ and β are the unimolecular and bimolecular recombination rates, respectively. From the Beer-Lambert law, we can relate n to the PIA signal ($\Delta T/T$) as:

$$n = \frac{-1}{\sigma d}\ln(1+\frac{\Delta T}{T}) . \quad (2)$$

Here σ (cm^2) is the polaron/triplet absorption cross section and d (cm) is the film absorption length. Equation (1) does not yield a unique photoexcitation population density that is independent of time during the entire relaxation process. We assume that G adopts a symmetric square-wave functional form to solve this equation under quasi-steady-state conditions. At quasi-steady-state conditions, equation (1) can be described by [35, 36]:

$$n_s = \frac{\kappa\rho \tanh\frac{\gamma\pi}{2\omega}\tanh\frac{P\pi}{\omega}}{\frac{\gamma}{2}\tanh\frac{P\pi}{\omega} + P\tanh\frac{\gamma\pi}{2\omega}}, \quad P = \sqrt{\beta\kappa\rho + \frac{\gamma^2}{4}}, \quad (3)$$

where, ω is the pump modulation angular frequency.

In order to extract the unique value for the parameters, we firstly consider the true steady-state situation (dn/dt=0) in order to suppress the dependence of n on γ and β. At high frequency compared to the relaxation lifetime, n is independent of recombination rates:

$$n = \frac{\kappa\rho}{4\pi\omega}, \quad (4)$$

Thus, we plot the product ($n\omega$) as a function of pump modulation frequency ($\omega/2\pi$) for triplets (a) and polarons (b) in one-phase and two-phase systems, shown in Fig. 4, and extrapolate this asymptotic product at high frequency to obtain the photoexcitation generation efficiency κ. Here, ρ=(1.20± 0.01)×10^{24} $cm^{-3}s^{-1}$. Polaron and triplet absorption cross sections are estimated as $\sigma_{triplet}$=1×10^{-15} cm^2 and $\sigma_{polaron}$=1×10^{-16} cm^2, which correspond to the values of other semiconductor polymers. [37] The extracted photogeneration efficiency values κ for these species are presented in Table 1. We conclude that (*i*) polarons are generated more efficiently than triplets in both systems at steady state, and (*ii*) triplets and polarons are generated more efficiently in finely intermixed systems compared to two-phase morphologies where the components are more phase-separated.

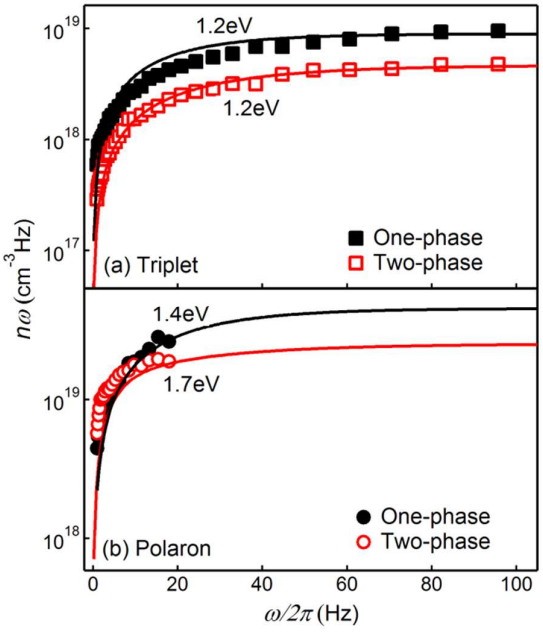

Fig. 4 Frequency dependence of the product of pump modulation angular frequency ω and photoexcitation density n of triplets (a) and polarons (b) for finely intermixed one-phase blends and relatively phase-pure systems where the fullerene and polymer are more pronouncedly phase separated, measured at 10 K. The full curves are fit to a function proportional to a×(2−exp(−x/b)−exp(−x/c)).

Next, we turn to the pump intensity dependence data to extract the unimolecular and bimolecular recombination rates γ and β. We plot the population density n as a function of ρ for polarons and triplets in one-phase and two-phase systems, shown in Fig. 5. The full lines are fit to equation (3) with the fixed generation efficiency κ. The extracted unimolecular recombination rate γ and bimolecular recombination rate β are presented in Table 1. The obtained values demonstrate that polarons generated in the finely intermixed, one-phase systems have higher recombination rates than those generated in two-phase systems.

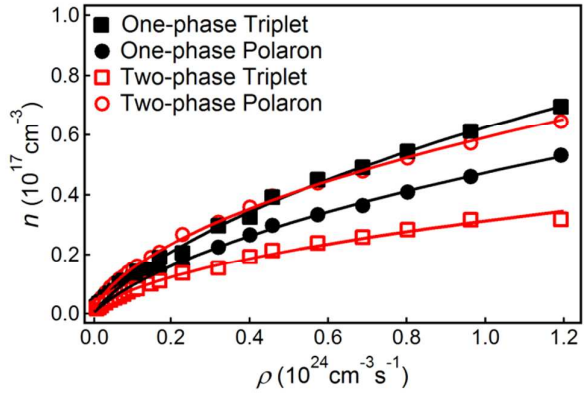

Fig. 5 Polarons and triplets densities (n) as a function of the density of pump photon per unit volume per unit time (ρ) in finely intermixed, one-phase systems and two-phase blends where the polymer and fullerene are more phase separated. The full curves are fits to equation (3).

Table 1 Summary of quasi-steady-state photo generation efficiencies (κ), unimolecular recombination rate (γ) and bimolecular recombination rate (β) extracted from fitting the pump modulation frequency dependence and pump modulation intensity dependence PIA data to equation (3) for polarons and triplets in finely intermixed one-phase and phase-pure polymer and fullerene two-phase systems. The errors represent one standard deviation of uncertainty from the fits to the data.

Materials	Species	σ (1×10^{-15} cm^2)	κ (1×10^{-4})	β (1×10^{-14} cm^3 s^{-1})	γ (1×10^{3} s^{-1})
pBTTT-C_{16}:PC_{61}BM (one-phase)	Polarons	0.1	9.40±0.012	26.0±0.96	7.58±0.32
	Triplets	1	1.86±0.016	2.85±0.14	1.20±0.06
pBTTT-C_{16} :Me12:PC_{61}M (two-phase)	Polarons	0.1	4.18±0.027	9.77±0.18	1.30±0.07
	Triplets	1	0.96±0.086	7.98±0.39	0.58±0.08

4. Discussion

We start our discussion based on the results generated from the combined quasi-steady-state PIA spectroscopy analysis of these two-phase morphologies and first summarise our observations.

(1) Quasi-steady state PIA spectroscopy shows that triplet excitons and polarons are generated in both intermixed one-phase systems as well as two-phase morphologies comprised of relatively pure domains of the two components. The triplet features are found at 1.2 eV for both morphologies, while the polarons features are at 1.4 eV in finely intermixed, one-phase systems and at 1.7 eV in two-phase systems, where the polymer and fullerene are phase separated.

(2) The photogeneration efficiency of polarons is larger than that of triplets in both systems at steady state, and the polarons and triplets generation efficiency in finely intermixed, one-

phase systems is higher than that in the blend structures comprising relatively phase-pure domains of the polymer and fullerene. This can be extracted from the fits to the model of the frequency-dependent quasi-steady-state PIA data.

(3) Both unimolecular recombination and bimolecular recombination are active in these two types of phase morphologies. The recombination rates in finely intermixed, one-phase systems are higher than in the two-phase systems. This is deduced by modelling the pump-intensity dependent PIA data.

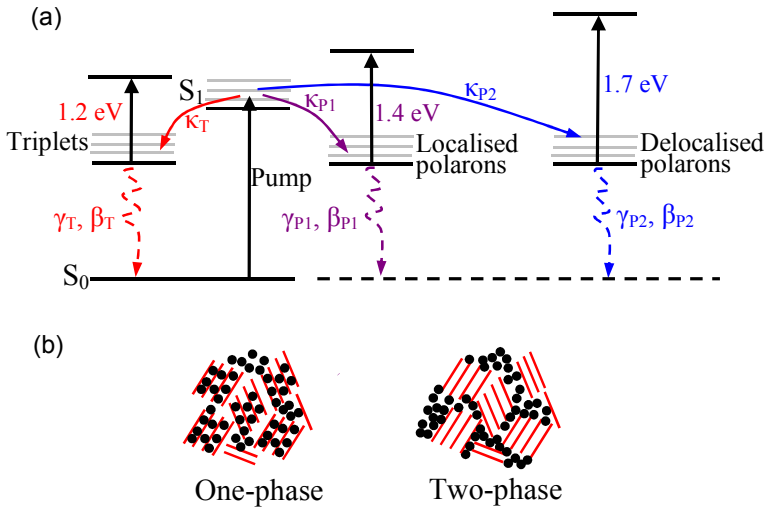

Fig. 6 (a) Energy levels and photoexcitations dynamics in finely intermixed, one-phase systems and two-phase (phase-pure polymer and fullerene) systems. S_0 and S_1 denote the ground state and the singlet excited state, respectively. Triplets, localised polarons, and delocalised polarons describe the long-lived photoexcitations generated by the pump excitation in both systems with the measured photoinduced photon energy and simulated generation and recombination rates adjacent to the dynamics. (b) Schematic representation of the two phase morphologies investigated here (see for a detailed structural analysis Ref. 16), where the $PC_{61}BM$ molecules are depicted with black symbols and pBTTT-C_{16} with red lines. The binary system (left) is predominately composed of a highly intermixed phase (the co-crystalline phase) with limited phase separation occuring, while addition of Me12 leads the fullerene and polymer to phase separate (right). This results into formation of large PCBM clusters that are visible in optical microscopy while also smaller-scale variations occur on the100 nm scale. [16]

Let us focus secondly on the different nature of polarons generated in one-phase and two-phase morphologies. To this end, we compare the quasi-steady-state PIA spectra of these two systems with neat pBTTT-C_{16} films (see Fig.7). In neat pBTTT films, triplets and polarons absorption energies are over a range of 0.7 eV to 1.65 eV, which is similar to the energy of polarons generated in the two-phase systems and ~250 meV higher than the energy of polarons in co-crystal structure. We propose that these two features are more highly localised (1.4 eV-peak) and more delocalised polarons (1.7 eV-peak) by comparison of these features to those in regioregular and regiorandom P3HT materials and as assigned by Österbacka *et al.*, who found that the photoinduced delocalised polarons have a higher energy than localised polarons. [21] These ideas are depicted in an energy level diagram of different photoexcitations in Fig. 6 (a), where we also included schematics of the phase morphologies of one-phase and two-phase systems (Fig.6 (b)). We emphasise that the polarons probed at 10 K are highly localised in that they are 'frozen' in a site that is near the photogeneration site, but 'localised' and 'delocalised' in this context refers to the spatial coherence in these otherwise trap sites.

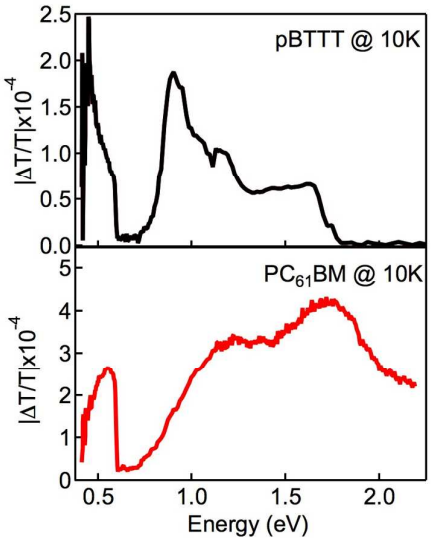

Fig. 7 The PIA spectra of neat polymer pBTTT and $PC_{61}BM$.

We draw our attention now to the respective generation and recombination kinetics of triplet excitons, localised and delocalised polarons and how they are influenced by the phase morphology. We have demonstrated that polarons are generated more efficiently than triplets in both systems. We have also shown that the long-lived photoexcitations are generated more efficiently in finely intermixed, one-phase systems compared to systems composed of relatively phase-pure domains of the pBTTT-C_{16} and fullerenes, highlighting that polarons are generated at molecular interfaces. Indeed, in the 1:1 pBTTT-C_{16}:PC_{61}BM binaries, the polymer and fullerene are intimately mixed at a molecular level. [16] On the other hand, in pBTTT-C_{16}:Me12:PC_{61}BM systems, the polymer and fullerene molecules are separated into relatively phase-pure domains, [16] reducing the generation efficiency. However, the higher generation efficiency in the co-crystal comes at the expense of higher recombination rates. Finally, from the spectral shift of the polaron absorption found for the intermixed, one-phase systems compared to the one observed for two-phase morphologies, we conclude that the polarons in the intermixed structures are more localised.

We now consider the overall effect of the generation and recombination kinetics of localised and delocalised polarons in order to discuss their steady-state density. We find that although the 1:1 pBTTT-C_{16}:PC_{61}BM co-crystal structures feature a higher polaron generation efficiency; they also exhibit rapid recombination losses due to the intimate intermixing of the polymer and fullerene, leading to shorter intermolecular distances and stronger Coulomb interactions between the holes and electrons. This reduces the yield of charge carriers at steady state, thereby preventing efficient charge collection. In contrast, systems, where the polymer and fullerene are phase separated, display lower polaron recombination rates compared to intermixed structures, especially for the unimolecular recombination, although this type of phase morphology produces lower polaron generation efficiency. It is however

important to note that because the polarons that are generated are more delocalised in such two-phase structures, we expect that these are more readily separated. Such a picture is consistent with reports by Niklas *et al.*, who found that the strong delocalisation of polarons from the polymer donor is critical for the efficient charge separation in polymers such as P3HT, PCDTBT and PTB7 when blended with $PC_{61}BM$ and $PC_{71}BM$. [38] Furthermore, our understanding also agrees well with the conclusions by Scarongella *et al.*, [17] who investigated the charge generation in 1:1 and 1:4 pBTTT-C_{16}:$PC_{61}BM$ blends, the latter featuring phase-pure $PC_{61}BM$ domains beside the co-crystal phase. Fast charge separation (on femtosecond to microsecond timescale) was observed in the finely intermixed, one phase systems formed by the 1:1 blend, in accord with the faster polaron generation efficiency (lager than hundreds of microseconds) we find in the same system. A slower charge generation rate was found for the 1:4 blends where the intermixed phase co-exists with $PC_{61}BM$ domains. This indicates that phase-pure domains limit charge generation efficiency – in the case of our pBTTT-C_{16}:Me12:$PC_{61}BM$ ternary, the rate constant is reduced by a factor of two compared to the finely intermixed, one-phase systems, as deduced from fitting the pump-intensity-dependent and pump-frequency-dependent photoinduced spectroscopy measurements with the quasi-steady state solution of a mesoscopic rate model. Note that we exclude any effect on the generation/recombination rates from the fact that we are using fatty acid methyl ester molecules as additives; previous studies indicated that Me12 do not remain in the pBTTT-C_{16}:Me12:$PC_{61}BM$ film after its fabrication [16]. This demonstrates that the delocalisation of polarons in crystalline solid solution systems can be controlled by tuning the phase separation of two components; here the different morphologies (highly intermixed vs. phase-separated) have been achieved by using suitable additives.

5. Conclusions

We have implemented quasi-steady-state photoinduced absorption spectroscopy to explore the nature of long-lived charges in pBTTT-C_{16}:$PC_{61}BM$ (one-phase, highly intermixed) and pBTTT-C_{16}:Me12:$PC_{61}BM$ (polymer and fullerene predominantly phase separated) systems. Polarons in the highly intermixed system are more localised than in the two-phase morphologies. Moreover, we found that in these two phase structures, the polaron generation efficiency is higher than the triplet-exciton generation efficiency. Finally, both the polaron generation efficiency and the recombination rate are higher in the one-phase pBTTT-C_{16}:$PC_{61}BM$ systems compared to the two-phase systems comprising Me12 as additive. Based on these observations we propose that the holes and electrons in delocalised polarons dissociate more readily and have lower probability to recombine compared to localised polarons. We consider that our observations are not limited to the specific case of pBTTT-C_{16}:fullerene blends but likely are generally applicable to other systems where multiple phases may co-exist depending on the chemical nature of the components and processing conditions selected.

Acknowledgements

CS acknowledges funding from the Natural Science and Engineering Research Council of Canada and the Canada Research Chair in Organic Semiconductor Materials; FD acknowledges funding through scholarships from the Royal Society K. C. Wang Postdoctoral Fellowship, the International Postdoctoral Exchange Fellowship Program, the Joint-PhD program founded by China Scholarship Council, and the Quebec's Ministère de l'Éducation, du Loisir, et du Sport (MELS); MS is supported by a postdoctoral fellowship from MELS; while NS is supported by a European Research Council (ERC) Starting Independent

Researcher Fellowship under the grant agreement No. 279587. This work furthermore was supported by KAUST through a Competitive Research Grant (CRG-1-2012-THO-015-IMP).

References

1 C. J. Brabec, M. Heeney, I. McCulloch and J. Nelson, *Chem. Soc. Rev.*, 2011, **40(3)**, 1185–1199.

2 Z. Ying, and J. Xue, *Polym. Rev.,* 2010, **50**, 420-453.

3 N. Stingelin, *Polymer International*, 2012, **61**, 866-873.

4 M. A. Brady, M. S. Gregory and L. C. Michael, *Soft Matt.,* 2011 **7**, 11065.

5 D. M. DeLongchamp, R. J. Kline, E. K. Lin, D. A. Fischer, L. J. Richter, L. A. Lucas, M. Heeney, I. McCulloch and J. E. Northrop, *Adv. Mater.*, 2007, **19**, 833.

6 M. Baklar, H. W. Paul, D. Sparrowe, M. Gonc, I. Mcculloch, M. Heeney and N. Stingelin, *J. Mater. Chem.*, 2010, **20**, 1927-1931.

7 B. H. Hamadani, D. J. Gundlach, I. McCulloch and M. Heeney, *Appl. Phys. Lett.*, 2007, **91**, 243512.

8 N. C. Cates, R. Gysel, Z. Beiley, C. E. Miller, M. F. Toney, M. Heeney, I. McCulloch, and M. D. McGehee, *Nano letters,* 2009, **9**, 4153-4157.

9 A. C. Mayer, M. F. Toney, S. R. Scully, J. Rivnay, C. J. Brabec, M. Scharber, M. Koppe, M. Heeney, I. McCulloch and M. D. McGehee, *Adv. Funct. Mater.*, 2009, **19**, 1173-1179.

10 J. G. Labram, E. B. Domingo, N. Stingelin, D. D. C. Bradley and T. D. Anthopoulos, *Adv. Funct. Mater.*, 2011, **21**, 356-363.

11 T. Agostinelli, S. Lilliu, J. G. Labram, M. Campoy-Quiles, M. Hampton, E. Pires, J. Rawle, O. Bikondoa, D. D. C. Bradley, T. D. Anthopoulos, J. Nelson and J. E. Macdonald, *Adv. Funct. Mater.*, 2011, **21**, 1701-1708.

12 A. M. Ballantyne, T. A. M. Ferenczi, M. Campoy-Quiles, T. M. Clarke, A. Maurano, K. H. Wong, W. Zhang, N. Stingelin-Stutzmann, J. -S. Kim, D. D. C. Bradley, J. R. Durrant, I. McCulloch, M. Heeney, J. Nelson, S. Tierney, W. Duffy, C. Mueller and P. Smith, *Macromolecules*, 2010, **43**, 1169-1174.

13 K. Maturova, S. S. van Bavel, M. M. Wienk, R. A. J. Janssen and M. Kemerink, *Adv. Funct. Mater.*, 2011, **21**, 261-269.

14 W. L. Rance, A. J. Ferguson, T. McCarthy-Ward, M. Heeney, D. S. Ginley, D. C. Olson, G. Rumbles and N. Kopidakis, *ACS Nano*, 2011, **5**, 5635-5646.

15 F. C. Jamieson, E. B. Domingo, T. McCarthy-Ward, M. Heeney, N. Stingelin, and J. R. Durrant, *Chem. Sci.,* 2012, **3**, 485.

16 E. Buchaca-Domingo, A. J. Ferguson, F. C. Jamieson, T. McCarthy-Ward, S. Shoaee, J. Tumbleston, N. Kopidakis, O. G. Reid, M. -B. Madec, M. Pfannmöller, R. R. Schröder, S. Watkins, G. Portale, F. Hermerschmidt, P. Smith, M. Heeney, H. Ade, G. Rumbles, J. R. Durrant, and N. Stingelin, *Mater. Horiz*. 2013, Nov. 22.

17 M. Scarongella, A. A. Paraecattil, E. Buchaca-Domingo, J. D. Douglas, S. Beaupré, T. McCarthy-Ward, M. Heeney, J.-E. Moser, M. Leclerc, J. M. J. Frećhet, N. Stingelin and N. Banerji, *J. Mater. Chem. A,* 2014, **2**, 6218-6230.

18 J. Rivnay, S. C. B. Mannsfeld, C. E. Miller, A. Salleo and M. F. Toney, *Chem. Rev.*, 2012, **112**, 5488.

19 T. J. Savenije, W. J. Grzegorczyk, M. Heeney, S. Tierney, I. McCulloch and L. D. A. Siebbeles, *J. Phys. Chem. C*, 2010, **114**, 15116-15120.

20 H. Kallel, G. Latini, F. Paquin, R. Rinfret, N. Stingelin and C. Silva, arXiv:1007.3035v2 [cond-mat.mtrl-sci].

21 R. Österbacka, C. P. An, X. M. Jiang and Z. V. Vardeny, *Science,* 2000, **287**, 839-842.

22 O. J. Korovyanko, R. Österbacka, X. M. Jiang, Z. V. Vardeny and R. A. Janssen, *J. Phys. Rev. B,* 2001, **64**, 235122.

23 M. Wohlgenannt, K. Tandon, S. Mazumdar, S. Ramasesha, Z. V. Vardeny, *Nature*, 2001, **409**, 494-7.

24 M. Wohlgenannt, X. Jiang, Z. V. Vardeny, R. Janssen, *Phys. Rev. Lett.*, 2002, **88**, 13–16.

25 M. Wohlgenannt, Z. V. Vardeny, *Synt. Met.*, 2002, **125**, 55–63.

26 M. J. Lee, Z. Y. Chen, R. di Pietro, M. Heeney, H. Sirringhaus, *Chem. Mater.*, 2013, **25**, 2075.

27 C. M. Pochas and F. C. Spano, submitted to *J. Chem. Phys.*, 2014.

28 I. I. Fishchuk, A. Kadashchuk, L. S. Devi, P. Heremans, H. Bässler, A. Köhler. Physical Review B, 2008, **78**, 045211.

29 S. T. Hoffmann, E. Scheler, J.-M. Koenen, M. Forster, U. Scherf, P. Strohriegl, H. Bässler, A. Köhler Physical Review B, 2010, **81**, 165208.

30 T. Kobayashi, K. Kinoshita, T. Nagase, and H. Naito, *Phys. Rev. B*, 2011, **83**, 1-7.

31 J. Poplawski, E. Ehrenfreund, J. Cornil, J. L. Bredas, R. Pugh, M. Ibrahim, A. J. Frank, *Mol. Cryst. Liq. Cryst. Sci. Technol. Sect. A*, 1994, **256**, 13.

32 O. Epshtein, Y. Eichen, E. Ehrenfreund, M. Wohlgenannt and Z. V. Vardeny, *Phys. Rev. Lett.,* 2003, **90**, 1-4.

33 C.-N. Brosseau, M. Perrin, C. Silva, R. Leonelli, *Phys. Rev. B*, 2010, **82**, 085305.

34 S. Gelinas, O. P.-Labrosse, C.-N. Brosseau, S. Albert-seifried, C. R. Mcneill, K. R. Kirov, I. A. Howard, R. Leonelli, R. H. Friend and C. Silva, *J. Phys. Chem. C*, 2011, **115**, 7114-7119.

35 G. Dellepaine, C. Cuniberti, D. Comoretto, G. F. Musso, G. Figari, A. Piaggi and A. Borghesi, *Phys. Rev. B,* 1993, **48**, 7850.

36 C. Silva, D. M. Russell, A. S. Dhoot, L. M. Herz, C. Daniel, N. C. Greenham, A. C. Arias, S. Setayesh, K. Müllen and R. H. Friend, *J. Phys.: Condens. Matter.,* 2002, **14**, 9803-9824.

37 C. Lee, X. Yang and N. Greenham, *Phys. Rev. B*, 2007, **76**, 245201-245207.

38 Jens Niklas, Kristy L. Mardis, Brian P. Banks, Gregory M. Grooms, Andreas Sperlich, Vladimir Dyakonov, Serge Beaupré, Mario Leclerc, Tao Xu, Luping Yue and Oleg G. Poluektov, *Phys. Chem. Chem. Phys.*, 2013, **15**, 9562.